

# Electrocatalytic Degradation of Sulfameth Thiadiazole by GAC@Ni/Fe Three-Dimensional Particle Electrode

Siwen Li

Northeast Normal University <https://orcid.org/0000-0002-4400-6661>

Yingzi Lin (✉ [linyingsi@jlu.edu.cn](mailto:linyingsi@jlu.edu.cn))

Jilin Jianzhu University <https://orcid.org/0000-0003-1792-4982>

SuiYi Zhu

Northeast Normal University

Gen Liu

Northeast Normal University

---

## Research Article

**Keywords:** Sulfamethylthiadiazole, GAC@Ni/Fe particle electrode, OH Contribution rate, Degradation pathway

**Posted Date:** November 29th, 2021

**DOI:** <https://doi.org/10.21203/rs.3.rs-1013267/v1>

**License:**   This work is licensed under a Creative Commons Attribution 4.0 International License.

[Read Full License](#)

---

# Abstract

In this work, GAC@Ni/Fe particle electrodes were prepared and employed for the degradation of Sulfamethylthiadiazole (SMT) by three-dimensional electrocatalytic technology. The effects of particle electrode bi-metal loading ratio, cell voltage, particle electrode dosage, electrode plate spacing and SMT initial concentration on SMT removal were studied. In addition, GAC@Ni/Fe particle electrode was analyzed by the scanning electron microscope (SEM), transmission electron microscope (TEM), X-ray diffractometer (XRD), X-ray photoelectron spectrometer (XPS) and Fourier transform infrared spectrometer (FTIR) to characterize. which indicated that a significant amount of Iron-nickel oxide were formed on the surface of GAC@Ni/Fe particle electrode. The results indicated that when the nickel-iron loading ratio is 1:1, the SMT removal effect is the best, and the removal rate can reach 90.89% within 30 minutes. Compared with the granular activated carbon without bimetal, the removal efficiency is increased by 37.58%. The degradation of SMT in the GAC@Ni/Fe particle three-dimensional electrode reactor is the joint result of both direct oxidation and indirect oxidation. The contribution rates of direct oxidation of anode and particle electrode and indirect oxidation of  $\cdot\text{OH}$  in the degradation are 32%, 27% and 41%, respectively. Based on the intermediate detected by ultra high liquid chromatography and the calculation of bond energy of SMT molecule by Gauss software, the degradation pathway of SMT in the GAC@Ni/Fe three-dimensional electrode reactor is proposed. This research provides a green, healthy and effective method for removing sulfonamide micro-polluted wastewater.

## 1. Introduction

In recent years, the widespread use of pharmaceuticals and personal care products (PPCPs) has greatly improved the healthy life of human beings, but it has also caused potential safety risks to the ecological environment and ecosystems (Kurade et al., 2021.; Lu et al., 2021.; Shahriar et al., 2021.; Yxc et al., 2021.; Chaturvedi et al., 2021). Water environment serves as one of the major pollution transmitting carriers of the emerging organic pollutants, and more and more PPCPs are also frequently detected in the water (Shannon et al., 2008.; Ying et al., 2021.; Ren et al., 2021.; Meng et al., 2021.; Chen et al., 2021.; Chen et al., 2020.; Yang et al., 2020), both of which have attracted wide attention from researchers.

PPCPs mainly include antibiotics, hormones, anti-epileptic drugs and personal care products such as preservatives, fungicides, disinfectants, etc. (Yi et al., 2017.; N. et al., 2019). They have the characteristics of high toxicity, strong bioaccumulation, and refractory biodegradability. In the environmental media they can be absorbed and enriched by the human body or other organisms (Zhang et al., 2020), causing the feminization of biological organisms, increasing the cancer rate of the reproductive system, destroying the immune system and central nervous system and other hazards (Jl et al., 2019). Among antibiotics, sulfonamides (Sulfonamides, SAs), as a common medicine for both humans and animals, has been used frequently as an important chemotherapeutic drug (Dumont et al., 2006), and its dosage accounts for more than 12% of the total types of antibiotics (Xu et al., 2009). The removal efficiency of SAs in sewage treatment plants is very low (Yi et al., 2017.; N. et al., 2019.; K Jüttner et al., 2000), due to the fact that by means of the traditional treatment process, it is difficult to effectively remove the sulfonamide organics in

the water (Yang et al., 2021.; Wang et al., 2016.; Dao et al., 2020.; Tarpani et al., 2018.; Samaras et al., 2013). Biological treatment technology requires many restrictions, the investment in operation and maintenance is large, and the effect is difficult to maintain for a long time (Oller et al., 2012). Physical and chemical methods are at high cost relatively and may cause secondary pollution and other risks. A majority of sulfonamides directly discharged into environment with the excrement of livestock and poultry and gradually accumulated in the groundwater due to its refractory property, and were detected in pig slurry (up to 500 mg/L), in surface water (up to 40 ng/L) and in groundwater (up to 20 ng/L) (Zhang et al., 2019), which caused serious environmental pollution including antibiotic resistance of bacterial pathogens and generation of superbacteria (Zhu et al., 2016; Teng et al., 2019). Therefore, it is an urgent demand to develop effective and economical methods for elimination of sulfonamide from wastewater to prevent water environment pollution (Liu et al., 2015; Muhammad et al., 2021).

In the past 20 years, the electrochemical method has been called clean processing technology due to its simple structure, small occupied area, and easy management (K Jüttner et al., 2000). In recent years the three-dimensional electrode system has been highly valued by scientific researchers. The three-dimensional electrode is the bipolar particles formed by filling with granular materials between the plates of the two-dimensional electrode electrolytic cell, and the filled particles are polarized under the action of an electric field. Each bipolar particle forms a micro electrolytic cell, and Hydroxyl radicals are generated on the surface of particle electrodes to undergo oxidation-reduction reactions with organics. These particle electrodes are usually some kind of granular or debris-like fillers. The choice of particle electrodes is also the key to design and improve the overall operating efficiency of the three-dimensional electrode system (Feng et al., 2015). The most common particle electrodes are metal particles, granular activated carbon (GAC) (Zhao et al., 2017.; Sun et al., 2014), carbon aerogel (GA), etc. (Zhuang et al., 2017.; Berenguer et al., 2010.; Zhang et al., 2013) .

Bimetallic catalysis has been widely concerned by researchers since the 1950s (Hai-Yan et al., 2018). Compared with single metal particles, bimetallic particles usually show higher catalytic activity (Chen et al., 2017). The reserve of metal nickel and iron in the earth is extremely abundant, and as a magnetic material, nickel is corrosion-resistant and has low cost. It can form a galvanic cell with iron to change the properties of ferroelectronics (Kuang et al., 2015.; Weng et al., 2014) and slow down its passivation (Lu et al., 2017.; Zhou et al., 2014.), both of which can effectively enhance the performance of each other, play a synergistic catalysis, and improve the performance of degrading organic pollutants (Gon?Alves et al., 2016.; Schrick et al., 2002.; Kadu et al., 2017).

In this study, GAC is used as the carrier, and the metal nickel and iron are loaded on the surface of the GAC by the liquid-phase reduction method to prepare a high-performance particle electrode with bimetallic synergistic catalytic function, which is used to degrade the typical SAs—sulfamethiazole (SMT). SEM, TEM, XRD, XPS, FTIR, etc. are used to characterize the particle electrode. Moreover, we discuss the synergistic catalysis of metal nickel's and iron's load ratio, the impact of key factors such as the initial voltage, particle electrode dosage, electrode plate spacing and SMT initial concentration on the degradation efficiency, so as to determine the optimal reaction conditions. The study also reveals the

mechanism and possible degradation pathways of electrocatalytic degradation of SMT, providing more theoretical basis for the degradation of SMT by the three-dimensional electrode reactor, and offering a research foundation to its wide application in the future.

## 2. Materials And Methods

### 2.1. Materials

Methanol ( $\text{CH}_3\text{OH}$ ) was purchased from Anhui Dadi High Purity Solvent Co., Ltd., acetic acid ( $\text{CH}_3\text{COOH}$ ) was purchased from Tianjin Komiou Chemical Reagent Co., Ltd., dilute sulfuric acid ( $\text{H}_2\text{SO}_4$ ) was purchased from Beijing Chemical Plant, absolute ethanol ( $\text{C}_2\text{H}_5\text{OH}$ ) was purchased from West Long Science Co., Ltd., ferrous sulfate heptahydrate ( $\text{FeSO}_4 \cdot 7\text{H}_2\text{O}$ ) and nickel chloride hexahydrate ( $\text{NiCl}_2 \cdot 6\text{H}_2\text{O}$ ) were purchased from Sinopharm Chemical Reagent Co., Ltd.; sodium borohydride ( $\text{NaBH}_4$ ) was purchased from Shandong West Asia Chemical Industry Co., Ltd. Company; granular activated carbon (GAC), nitrogen ( $\text{N}_2$ ), and sulfamethiadiazole (SMT) were purchased from Yuanye Biology; tert-butanol ( $\text{C}_4\text{H}_{10}\text{O}$ ) was purchased from Tianjin Guangfu Fine Chemical Research Institute; and experimental water was deionized water, etc.

### 2.2 Preparation of GAC@Ni/Fe particle electrodes

The granular activated carbon was soaked in 0.05mol/L dilute sulfuric acid for 30 minutes, after being filtered it was washed with ethanol solution and deionized water for three times, and then dried in a constant temperature drying oven at 105°C for 10 hours, sealed and stored for later use.

Weigh an appropriate amount of  $\text{FeSO}_4 \cdot 7\text{H}_2\text{O}$  and  $\text{NiCl}_2 \cdot 6\text{H}_2\text{O}$  and dissolve them in a certain amount of deionized water, and stir until they are completely dissolved (the mass ratio of nickel and iron in the mixed solution is 2:1, 1:1, 1:2, respectively). The mixed solution was transferred to a 500mL three-necked flask containing an appropriate amount of pre-treated GAC. Under the protection of nitrogen, the newly prepared  $\text{NaBH}_4$  solution was added dropwise to the mixed solution of nickel and iron at a rate of 1 drop per second before completely stirring. The reduction reaction generated a supported nickel-iron bimetallic particle electrode, which was quickly filtered after full reaction, and placed in a drying oven for drying at 80°C for 10 hours for later use (Liu et al., 2012).

### 2.3 Construction of three-dimensional electrode filter system

The experimental devices of this study are shown in Figure 1. Three-dimensional electrode electrochemical reactor, including water inlet unit, peristaltic pump, main reaction unit, effluent collection unit, stirring system, cathode (graphene electrode), anode (ruthenium-iridium coated titanium electrode), particle electrode (self-made nickel-iron double metal particle electrode), DC power supply, water inlet and outlet valves, etc. The main reaction unit is equipped with an electrode card slot, which can control the distance between the positive and negative electrodes and set the particle electrode filling slot.

## 2.4 Analysis methods

Scanning electron microscopy (ZEISS SIGMA 500, SEM) and transmission electron microscopy (FEI Tecnai F30) characterization methods were used to analyze the surface morphology and element composition of the particle electrode, Fourier infrared spectroscopy (Perkin-Elmer Spectrum GX) was used to characterize the change of surface functional groups of the particle electrode after loading; X-ray diffractometer (X Pert-Pro MPD) was used to characterize the crystal structure of the particle electrode; X-ray photoelectron spectrometer (Thermo 250XI) was used to analyze the valence state of the bi-metal on the surface of the particle electrode; liquid chromatograph (Agilent 1260 Infinity II) was used to detect the concentration before and after the SMT reaction; a high-resolution mass spectrometer (Waters Q-TOF SYNAPT G2, USA) was used to analyze the degradation pathway.

## 2.5 SMT degradation experiment

In order to study the optimal reaction conditions of the GAC@Ni/Fe particle electrode electrocatalytic oxidation degradation of SMT, a single factor experiment was used to control the initial cell voltage, electrode plate spacing, particle electrode dosage and SMT initial concentration as the key variants of influencing factors to study the degradation efficiency. And in order to eliminate the influence of adsorption, adsorption experiments were carried out on the particle electrode before the experiment, and electrolysis experiments were carried out after the adsorption was saturated. The initial test conditions: cell voltage was 5V, electrode plate spacing was 1 cm, particle electrode dosage was 3g, and SMT initial concentration was 1mg/L.

## 3. Results Adn Discussion

### 3.1 Preparation of GAC@Ni/Fe particle electrodes

Under the experimental conditions of 2.5, the electrolyte was 0.01mol/L sodium sulfate ( $\text{Na}_2\text{SO}_4$ ) solution, and the degradation effects of two-dimensional electrodes and three-dimensional electrodes were compared. As shown in Figure 2a, within 30 minutes, the degradation rate of the three-dimensional electrode was 90.89%, being significantly better than that of the two-dimensional electrode at 29.34%. It is mainly attributed to the formation of tiny electrolytic cells for each particle electrode added, which increased the effective reaction area, improved the mass transfer efficiency of the reaction, and reduced the reaction distance so as to raise the generation of  $\cdot\text{OH}$  and improve SMT degradation efficiency.

#### 3.1.1 Effect of active components on SMT removal rate

The active catalytic components loaded by the particle electrode also have an important influence on the electrocatalytic performance of the particle electrode(Wang et al., 2008.). Figure 2a shows the effect of electrocatalytic degradation of SMT by particle electrodes loaded with different active ingredients. Under the same experimental conditions, the degradation performance of the unloaded particle electrode is significantly lower than that of the particle electrode loaded with metal active ingredients. The metal

active components increase the catalytic performance of the particle electrode; compared with the single metal, the bimetallic load represents a higher synergistic catalytic activity. The bi-metal also promotes each other to form a galvanic cell, which enhances each other's performance and improves the degradation efficiency.

### 3.1.2 Effect of Ni/Fe mass ratio on SMT removal rate

Figure 2b shows the effect of Ni/Fe loading mass ratio on the degradation of SMT in a three-dimensional electrode reactor. Under the same experimental conditions, the quality of ferronickel changes from 1:2 to 2:1, the degradation efficiency changes from 85.36–70.2%, and the maximum is reached when the mass ratio of ferronickel is 1:1, while the degradation rate is 90.89% in 30 minutes. The loaded bimetallic material promotes the degradation efficiency, but too much nickel or iron will produce side reactions that inhibit free radicals, so as to affect the synergistic catalysis and reduce the reaction efficiency. This study shows that when the mass ratio of nickel to iron is 1:1, the synergistic catalytic performance is the best. Therefore, the particle electrode is selected under this ratio in the single factor research experiment.

## 3.2 Physical and chemical properties of GAC@Ni/Fe granular electrode

### 3.2.1 SEM characterization

Scanning electron microscope is used to observe the unloaded GAC particle electrode and GAC@Ni/Fe particle electrode, and the results are shown in Figure 3a,b. The surface of GAC without metal loading has less impurities, and is loose and porous; the surface of the particle electrode after loading nickel-iron bi-metal presents a spherical structure with pleated "petal-shaped" flakes, which are evenly distributed on the GAC surface. The average diameter of the spherical particles is about 4.77 $\mu$ m. This pleated structure increases the specific surface area of the particle electrode and enhances the mass transfer performance of the material. The quantity of reactive sites increases, and the particle electrode better contacts the target pollutants, making it have better degradation performance(Zhang et al., 2020).

### 3.2.2 TEM-EDS characterization

In order to better analyze the apparent morphology and element composition of the particle electrode after loading, a transmission electron microscope is used to scan the homemade GAC@Ni/Fe particle electrode. As shown in Figure 3c, the boundary of the particle electrode particles is clear and smooth, showing a transparent state. It shows that the ultra-thin characteristics of petal-like nanosheets(Huang et al., 2014) are consistent with the SEM results. Figure 3d is the HRTEM figure of the GAC@Ni/Fe particle electrode, which shows different visible lattice fringes, which are 0.205nm, 0.247nm, 0.328nm and 0.239nm, respectively, corresponding to the crystal planes of Fe<sub>3</sub>O<sub>4</sub> (311), Ni<sub>2</sub>O<sub>3</sub>, FeO (104) and NiO (200) separately. And through EDS analysis, the percentage increase of nickel after loading is the same with that of iron, and they are evenly distributed on the GAC surface. The loading effect is better. In addition to

the detection of nickel, iron, and carbon, the peaks corresponding to oxygen also appear in the EDS spectrum. Part of the oxygen element comes from the GAC carrier, and the other part is caused by the oxidation of the nanoparticles during the processes of washing, drying and testing.

### 3.2.3 XRD characterization

Figure 4a is an analysis graph of the crystal form after the particle electrode is loaded with nickel and iron. It can be seen from the figure that a broad peak appears when the diffraction angle is  $2\theta = 26.6^\circ$ , which is the main peak of the graphite crystal form of granular activated carbon. The material shows the characteristic peak of iron oxide when the diffraction angle is  $2\theta = 36.820^\circ$  and  $2\theta = 60.694^\circ$  each, and the characteristic peak of nickel oxide appears at diffraction angles of  $2\theta = 44.832^\circ$  and  $2\theta = 43.275^\circ$ ; the main body of the particle electrode is composed of GAC, and the bi-metal is later loaded, only attached on the surface. Combined with the EDS analysis, the content of iron and nickel is relatively less, so their characteristic peak display and degree of crystallinity are not so obvious as those of the C element.

### 3.2.4 XPS characterization

XPS is mainly used to analyze the element composition and valence state distribution on the surface of the particle electrode after loading. From Figure 4b the full spectrum we can see that the surface of the particle electrode after loading mainly contains carbon, oxygen, iron, nickel and other elements. Among them, the particle electrode uses GAC as the carrier, which is the main source of carbon. Oxygen is caused by the long-term exposure of particles in the air and the oxidation of metal elements in the preparation process. It can be seen from the high-resolution spectrum of Fe 2P in Figure 4c that the binding energies of 714.7eV and 712.4eV, 725.4eV represent the characteristic peaks of  $\text{Fe}^{2+}$  and  $\text{Fe}^{3+}$  oxides respectively; from the high-resolution spectrum of Ni 2P in Figure 4d, it can be concluded that the binding energies of 855.6eV, 856.9eV, 861.8eV, 864.1 and 880.5 are all the characteristic peaks and satellite peaks of  $\text{Ni}^{2+}$  oxide, and 874.3eV is the characteristic peak of  $\text{Ni}^{3+}$  oxide. The results show that iron and nickel were successfully loaded on the GAC and formed a metal oxide layer.

### 3.2.5 IR characterization

Infrared spectroscopy is used to analyze the changes in surface functional groups before and after the particle electrode was loaded. The type and strength of the functional groups on the surface of the GAC@Ni/Fe particle electrode have changed significantly compared with that of GAC. The GAC wave number has a broad peak at  $3400.00\text{cm}^{-1}$ , which is attributed to the tensile vibration of the hydrogen-bonded OH group, and there is a small amount of bound water inside the polymer. After loading, The absorption peak at the wave number of  $1094.00\text{cm}^{-1}$  is generally considered to be the  $\text{-C=O}$  stretching vibration or  $\text{-C=C}$  stretching vibration of phenol, ether or alcohol; the corresponding peak at the wave number of  $1384.38\text{cm}^{-1}$  indicates the deformation vibration peak of the C-OH bond; the wave number at the  $1454.39\text{cm}^{-1}$  corresponds to the  $\text{-CH}_2$  scissors bending vibration peak. The increase of oxygen-containing functional groups and the abundant chemical groups on the surface also play an important role in the absorption and loading of nanomaterials(Zheng et al., 2014).

## 3.3 The influence of key factors on SMT degradation

The removal of organic pollutants by three-dimensional electrode reactor in the water mainly depends on the action of voltage, electrodes and catalytic particle electrodes, and generating  $\cdot\text{OH}$  oxidation groups, which decompose them into non-toxic and harmless substances like  $\text{CO}_2$  and  $\text{H}_2\text{O}$ , etc. In order to determine the optimal process conditions for the process for SMT, the main influencing factors on the degradation of SMT in the GAC@Ni/Fe three-dimensional particle electrode reactor were studied and analyzed.

### 3.3.1 The influence of cell voltage on SMT removal efficiency

Energy consumption is one of the important factors that restrict the prospects of electrochemical applications. The application of voltage during the degradation process directly determines the level of energy consumption. This research experiment is carried out under low voltage conditions, whose voltage range is 1-5V, and the main consideration is to save energy and prevent excessive voltage from breaking down the electrode. The effect of cell voltage in the GAC@Ni/Fe three-dimensional particle electrode reactor on the removal of SMT is studied through single factor experiments. Other experimental conditions are described in 2.5, and the experimental results are shown in Figure 5a. The voltage has a great influence on the removal effect of SMT. When the voltage is 1V, the degradation rate within 30 minutes is only 58.3%. When the voltage is increased to 5V, the degradation rate rapidly increases to 96.5%. The rise in cell voltage affects the distribution of power fields in the reactor, and the increase of the driving force after the particle electrode is re-polarized(Xiong et al., 2003) is one of the main factors for the improvement of the degradation effect.

Figure 5b shows the kinetic fitting curves of the degradation of SMT in the GAC@Ni/Fe three-dimensional particle electrode reactor under different cell voltages. The degradation process conforms to the Langmuir-Hinshelwood (L-H) pseudo-first-order reaction kinetic model. In addition, the reaction kinetics equations and rate constants related to this process are shown in Table 1. In the test range, the reaction rate constant increases with the rise of the voltage. The degradation efficiency is the best when the voltage is 5V, and the low voltage can ensure that the system has a high degradation efficiency.

Table 1

Reaction kinetic parameters of GAC@Ni/Fe particle electrode three-dimensional electrocatalytic system for degradation of SMT under different cell voltages

Cell Voltage	pseudo-first-order reaction kinetic model	rate constants( $\text{min}^{-1}$ )	correlation coefficient $R^2$
1V	$Y=0.02701x+0.04529$	0.02701	0.97257
2V	$Y=0.03997x+0.12283$	0.03997	0.95505
3V	$Y=0.05938x+0.35888$	0.05938	0.87338
4V	$Y=0.07275x+0.42937$	0.07275	0.89383
5V	$Y=0.08035x+1.18499$	0.08035	0.54933

### 3.3.2 The influence of particle electrode dosage on SMT removal efficiency

From Figure 5c, we can see that with the conditions of other test conditions unchanged, when the dosage of particle electrode is changed from 1g to 5g, the degradation rates are 66.6%, 87.5%, 99.9%, 97.5% and 99.3% respectively; with the increase of the particle electrode, the degradation efficiency increases significantly, reaching the maximum at 3g. The degradation effect of the particle electrode takes on slight fluctuations when particle electrode continues to be added, mainly because too many particle electrodes are filled in the electrode plates with a certain distance, which causes the particle electrode to accumulate and congest, and contact between the positive and negative electrodes increases the short-circuit current, causing the reaction current to fluctuate, which has a little impact on the degradation effect.

Figure 5d shows the kinetic curve fitting of the degradation of SMT in a three-dimensional electrode reactor under different particle electrode dosages. The degradation process conforms to the LH pseudo-first-order kinetic model. The related reaction kinetic equations and reaction rate constants are shown in the following table: with the increase of the particle electrode dosage, the reaction rate constant increases first and then decreases, and gradually stabilizes. When the dosage is 3g, the reaction rate is the largest. Therefore, 3g is the most suitable dosage in this volume and degradation system.

Table 2

Reaction kinetic parameters of GAC@Ni/Fe particle electrode three-dimensional electrocatalytic system for degradation of SMT under different particle electrode dosages

Particle electrode dosage	pseudo-first-order reaction kinetic model	rate constants( $\text{min}^{-1}$ )	correlation coefficient $R^2$
1g	$Y=0.03592X+0.09878$	0.03592	0.96384
2g	$Y=0.06996X-1.35750$	0.06996	0.98164
3g	$Y=0.22907X-0.36435$	0.22907	0.97274
4g	$Y=0.11625X-0.04426$	0.11625	0.96110
5g	$Y=0.14872X-0.02857$	0.14872	0.94417

### 3.3.3 The influence of electrode plate spacing on SMT removal efficiency

In order to discuss the influence of the distance between the electrode plates on the degradation effect of SMT, the experimental conditions are as shown in 2.5, by changing the distance between the two electrode plates. It can be seen from Figure 5e that when the electrode plate spacing is 0.5cm, the degradation effect is very low. Within 30 minutes, only 45.9% of the target pollutants are removed, mainly because of the too small electrode plate spacing, the negative electrode contact increases the short-circuit current, which causes the reaction current to rapidly decrease and the degradation efficiency of the system to decrease. When the plate spacing is increased, the system gradually recovers its performance. When the electrode plate spacing is 1cm–2.5cm, the degradation efficiency within 30 minutes is 93.8%, 90.0%, 99.3% and 91.0%, respectively. A short distance can reduce material diffusion and promote mass transfer(Lin et al., 2013), but a too small distance will result in excessive electric field strength, which may cause instantaneous discharge of the electrode plate when the power is turned on; when the impressed voltage is unchanged, the too large distance between the electrode plates will also increase the intensity of the electric field between the electrode plates, resulting in a decrease in the reaction current, thereby affecting the degree of re-polarization of the particle electrode(Shen et al., 2017). When the distance between the electrode plates is 2cm, it is more moderate and the degradation efficiency is the best. Therefore, in this study, the best electrode plate spacing is 2cm.

Figure 5f shows the kinetic curve fitting of the degradation of SMT in a three-dimensional electrode reactor with different electrode plate spacing. The degradation process conforms to the LH pseudo-first-order kinetic model. The related reaction kinetic equations and reaction rate constants are shown in the following table. When the electrode plate spacing is 2cm, the reaction rate reaches the maximum.

Table 3

Reaction kinetic parameters of GAC@Ni/Fe particle electrode three-dimensional electrocatalytic system for degradation of SMT with different electrode plate spacings

Plate spacing	pseudo-first-order reaction kinetic model	rate constants( $\text{min}^{-1}$ )	correlation coefficient $R^2$
0.5cm	$Y=0.01690x+0.17011$	0.01690	0.73832
1.0cm	$Y=0.08388x+0.45864$	0.08388	0.90225
1.5cm	$Y=0.06558x+0.49639$	0.06558	0.83883
2.0cm	$Y=0.15225x+0.39037$	0.15225	0.88535
2.5cm	$Y=0.07240x+0.54689$	0.07240	0.82873

### 3.3.4 The influence of SMT initial concentration on SMT removal efficiency

The experimental conditions are as 2.5, on the basis of not changing other conditions, the initial concentration of SMT increases from 1mg/L to 5mg/L. The result is shown in Figure 5g. In general, as the concentration of pollutants increases, the degradation efficiency and reaction rate constant of SMT gradually decrease. In theory, increasing the initial concentration of wastewater can reduce the limitation of mass transfer, thereby increasing the degradation efficiency. But the opposite results show that the degradation of SMT is not mainly controlled by electrochemical reaction. The increase of initial concentration inhibits the progress of the reaction, mainly because SMT contains refractory functional groups such as benzene ring(Chen et al., 2019), but has relatively slight effect on the degradation of SMT by means of GAC@Ni/Fe three-dimensional particle electrode system. It shows that the three-dimensional particle electrode is more suitable for effective removal of low-concentration pollutants. The concentration of SAs in natural water bodies is also relatively low, so this method is suitable for efficient removal of them.

Figure 5h shows the kinetic curve fitting of the degradation of SMT in a three-dimensional electrode reactor with different initial concentrations. The degradation process conforms to the LH pseudo-first-order kinetic model. The related reaction kinetic equations and reaction rate constants are shown in the following table. The degradation effect is best when the initial concentration is 1mg/L. The concentration of PPCPs in the water environment is generally at the level of ng/L- $\mu\text{g/L}$ , so this method can effectively degrade pollutants in the water environment.

Table 4

Reaction kinetic parameters of GAC@Ni/Fe particle electrode three-dimensional electrocatalytic system for degradation of SMT with different SMT initial concentrations

Initial concentration	pseudo-first-order reaction kinetic model	rate constants( $\text{min}^{-1}$ )	correlation coefficient $R^2$
1mg/L	$y=0.09685x+1.26016$	0.09685	0.69049
2mg/L	$y=0.07373x+0.74246$	0.07373	0.82289
3mg/L	$y=0.07678x-0.59100$	0.07687	0.90382
4mg/L	$y=0.06510x-0.51146$	0.06510	0.89302
5mg/L	$y=0.07201x-0.52601$	0.07201	0.90289

## 3.4 Research on SMT degradation mechanism and pathway

### 3.4.1 Analysis of degradation mechanism of three-dimensional electrode

In order to prove the role of  $\cdot\text{OH}$  in this experiment, tert-butanol is used as a quencher to inhibit the production of  $\cdot\text{OH}$ , so as to discuss the role of direct oxidation and indirect oxidation in this study(Sun et al., 2019). The effect of tert-butanol dosage on SMT removal rate is shown in Figure 6a. The results show that when the dosage of tert-butanol is 20mg/L, the degradation efficiency of the three-dimensional electrode reactor within 30 minutes decreases from 90.89–68.63%; when the dosage of tert-butanol is 100mg/L, it decreases to 57.78%; when the tert-butanol is continually added to be excessive, the degradation rate tends to be stable and no longer decreases significantly, and the degradation efficiency of SMT within 30 minutes is 53.65%. The above experiments prove that there is indeed the production of  $\cdot\text{OH}$  during the electrolysis process, and  $\cdot\text{OH}$  has a strong ability to oxidize and degrade SMT. In addition to the indirect oxidation of  $\text{OH}$ , oxidation reactions occur to the main electrode (anode) and the particle electrode, and the charge transfer among them effectively degrades SMT(Zhang et al., 2016.). The experiments also show that in addition to hydroxyl radicals, SMT also has direct oxidation and another degradation mechanism in the degradation process. Thus, the effective degradation of SMT in the GAC@Ni/Fe three-dimensional particle electrode reactor is the synergistic result of both direct oxidation and indirect oxidation(Wang et al., 2017). The main reaction mechanism is shown in Figure 6b. Combined with the research and analysis of 3.1.1, the bimetallic catalytic particle electrode plays a key role in the degradation process. The nickel-iron bi-metal shows higher degradation performance. Although the increase of nickel fails to enhance the formation of hydroxyl radicals, in the neutrality condition, the loading of Ni-Fe on the surface of the particle electrode promotes the oxidation of ferrous ions to produce a catalyst under aerobic conditions(Lee et al., 2008). In the two-dimensional electrode system, the degradation rate of SMT within 30 minutes is 29.34%, which is mainly the result of anodizing. The degradation rate within 30 minutes in the three-dimensional electrode system is 90.89%, which is a combination result of anodizing, particle electrode oxidation and the generated  $\cdot\text{OH}$ . The degradation rate of SMT within 30 minutes is 53.65% in the quenching test. Therefore, the calculations show that in the degradation of SMT in the GAC@Ni/Fe three-dimensional particle electrode electrocatalytic system, the

contribution rates of direct oxidation of anode, particle electrode oxidation and  $\cdot\text{OH}$  are 32%, 27% and 41%, respectively.

## 3.4.2 Possible products and degradation pathways of SMT

At present, there are few studies on the intermediate products of SMT degradation in three-dimensional electrode reactors. In order to better understand the degradation process of catalyzing and oxidizing SMT by GAC@Ni/Fe three-dimensional particle electrode, the intermediate products in the reaction process are identified by mass spectrometry technology. The possible products are shown in Figure 7, and the intermediate fragment ions of the mass spectrum are 76, 115, 140, 157, 172, 194, 217, and 248. The study first used the 6-31G basis set under the b3lyp theory to optimize the configuration of the SMT, and calculated the NBO charge, so as to further calculate the size of the compression Fukui function of each atom in the molecule, and combined it with the molecular electrostatic potential energy figure (See Supplementary Material) to indicate the interaction force between molecules. The red area represents negative charge and electrophilic correlation, and the blue area represents positive charge and nucleophilic correlation. The greater the color extent is, the greater the trend will be. To sum up, it is judged that when  $\cdot\text{OH}$  attacks SMT molecules, the reaction active sites are prone to appear, the amino groups on the benzene ring and the vicinity of the S-O bond, C-S bond and S-N bond are more likely to be attacked and have bond-breaking reactions. As shown in Figure 8, it is speculated that there are mainly two reaction pathways as follows. Firstly, through pathway 1  $\cdot\text{OH}$  attacks the nitrogen atoms in the amino groups on the benzene ring to form free radicals centered on N. The free radical cations undergo rapid and reversible hydration to produce aniline free radicals. These free radicals are further neutralized by oxygen molecules, resulting in the hydrolysis of hydroxylamine to nitro; at the same time,  $\cdot\text{OH}$  also attacks the C-S bond and S-N bond, etc., forming intermediate fragment ions 76, 115, 140, 157, 172, and 194, consistent with the results of mass spectrometry; in pathway 2,  $\cdot\text{OH}$  attacks the N-N bond and C-S bond on the five-membered heterocycle, forming intermediate fragment ions of 217 and 248. Finally, through a series of oxidation reactions, these molecules will eventually be mineralized and converted into inorganic substances, such as  $\text{CO}_2$  and  $\text{H}_2\text{O}$ , etc.

## 4 Conclusion

In this research work, GAC is used as the carrier, and the liquid-phase reduction method is adopted to prepare GAC@Ni/Fe particle electrode with bi-metal synergistic catalytic function to degrade SMT. When the mass ratio of nickel to iron is 1:1, the synergistic catalysis of the particle electrode has the best degradation performance. The SEM and TEM images show the morphology and structure of the GAC@Ni/Fe particle electrode. EDS, XPS, XRD and IR analyze the chemical combination and characteristics of the particle electrode, which proves the successful loading of nickel and iron bimetals and they exist in the form of oxides. The single factor experiment shows that when the cell voltage is 5V, the particle electrode dosage is 3g, electrode plate spacing is 2cm, and SMT initial concentration is 1mg/L, the degradation effect is best, conforming the first order kinetics, the removal efficiency of SMT can be stabilized above 90% within 30 minutes. The degradation of SMT in the GAC@Ni/Fe three-

dimensional particle electrode reactor is the joint result of both direct oxidation and indirect oxidation. ·OH is the major factor of degradation, while oxidation anode and particle electrode are the minor factors, whose contribution rates are 41%, 32%, and 27%, respectively. Through Gaussian calculations and mass spectrometry techniques, it is analyzed that in the degradation process, ·OH attacks the amino groups on the benzene ring and the S–O bond, C–S bond, and S–N bond for cleavage reactions, and proposes two possible degradation pathways of SMT. This study prepares GAC@Ni/Fe particle electrode with good performance, and realizes the effective degradation of SMT by constructing a three-dimensional electrode reaction system, which promotes the application of the three-dimensional electrode reactor, and provides new ideas for removal of the micro-polluted SAs pollutants in the water body.

## Declarations

### Ethics approval and consent to participate

Not applicable

### Consent for publication

Not applicable

### Availability of data and materials

The datasets used and/or analysed during the current study are available from the corresponding author on reasonable request.

### Competing interests

The authors declare that they have no competing interests

### Funding

Our work was supported by the National Natural Science Foundation of China (Grant No. 51778267), the National Water Pollution Control and Treatment Science and Technology Major Project (No. 2012ZX07408001), the Jilin Province Science and Technology Department Project (No. 20190201113JC), the Jilin Provincial Department of Ecology and Environment Project(No.2019-15).

### Authors' contributions

Siwen Li:writing, Methodology,Yingzi Lin:funding support, reviewing,Suiyi Zhu:reviewing,Gen Liua: Methodology

## References

1. Berenguer R, Marco-Lozar JP, Quijada C, D, Cazorla-Amorós & E Morallón. ,2010. Electrochemical regeneration and porosity recovery of phenol-saturated granular activated carbon in an alkaline medium. *Carbon*, 48(10),2734–2745
2. Zhang C, Jiang Y, Li Y, Hu Z L Zhou, & M Zhou.,2013. Three-dimensional electrochemical process for wastewater treatment: a general review. *CHEM ENG J*
3. Chaturvedi P, Shukla P, Giri BS, Chowdhary P, & Pandey A (2021) Prevalence and hazardous impact of pharmaceutical and personal care products and antibiotics in environment: a review on emerging contaminants. *ENVIRON RES*
4. Chen G, Zou N, Chen B, Sambur JB, Choudhary E, Chen P ,2017. Bimetallic effect of single nanocatalysts visualized by super-resolution catalysis imaging. *ACS Central Science*, 3(11),1189–1197
5. Chen H, Chen W, Guo H, Lin H, Zhang Y ,2021. Pharmaceuticals and personal care products in the seawater around a typical subtropical tourist city of china and associated ecological risk. *ENVIRON SCI POLLUT R*(18)
6. Chen H, Feng Y, Suo N, Long Y, Li X, & Shi Y et al 2019. Preparation of particle electrodes from manganese slag and its degradation performance for salicylic acid in the three-dimensional electrode reactor (tde). *Chemosphere*, 216(FEB.), 281-288
7. Chen L, Fu W, Tan Y, Zhang X ,2020. Emerging organic contaminants and odorous compounds in secondary effluent wastewater: identification and advanced treatment. *J HAZARD MATER*, 408(18),124817
8. Dao KC, Yang CC, Chen KF, Tsai YP ,2020. Recent trends in removal pharmaceuticals and personal care products by electrochemical oxidation and combined systems. *Water*, 12(4)
9. Dumont V, Huet AC, Traynor I, Elliott C, Delahaut P (2006) A surface plasmon resonance biosensor assay for the simultaneous determination of thiamphenicol, florefenicol, florefenicol amine and chloramphenicol residues in shrimps. *ANAL CHIM ACTA* 567(2):179–183
10. Feng Y, Wang X, Qi J, Wang Z, Li X ,2015. Production of red mud particle electrodes (rmpes) and its performance investigation in a biological aerated filter coupled with a three-dimensional particle electrode reactor (baf-tde). *IND ENG CHEM RES*, 54(26),150609060833000
11. Gonçalves AA, Araújo, Mesquita AF, Pires JD, Verly M, Silva LMD et al 2016. Characterisation of silica-supported Fe–Ni bimetallic nanoparticles and kinetic study of reductive degradation of the drug nimesulide. *Journal of Environmental Chemical Engineering*, 4(4),4354–4365
12. Hai-Yan YU, Dong-Kui LI, Wang N ,2018. Research progress of Fe-Ni bimetallic catalyst. *Yinshan Academic Journal*(Natural Science Edition)
13. Huang G, Zhang F, Zhang L, Du X, Wang J, Wang L (2014) Hierarchical NiFe<sub>2</sub>O<sub>4</sub>/Fe<sub>2</sub>O<sub>3</sub> nanotubes derived from metal organic frameworks for superior lithium ion battery anodes. *J MATER CHEM A* 2(21):8048
14. Ji A, Xh B, Bwb C, Qz A, Lc A, Lcc A (2019) Physico-chemical and biological aspects of a serially connected lab-scale constructed wetland- stabilization tank-gac slow sand filtration system during

- removal of selected ppcps. CHEM ENG J 369:1109–1118
15. Jüttner, Galla K, Schmieder H, 2000. Electrochemical approaches to environmental problems in the process industry., 45(15-16), 2575–2594
  16. Kadu BS, Wani KD, Kaul-Ghanekar R, Chikate RC (2017) Degradation of doxorubicin to non-toxic metabolites using Fe-Ni bimetallic nanoparticles. CHEM ENG J, 715–724
  17. Kuang Y, Du J, Zhou R, Chen Z, Megharaj, Mallavarapu Naidu, Ravendra, 2015. Calcium alginate encapsulated Ni/Fe nanoparticles beads for simultaneous removal of Cu(II) and monochlorobenzene. Journal of Colloid & Interface Science, 447, 85–91
  18. Kurade MB, Ha YH, Xiong JQ, Govindwar SP, & Jeon BH (2021) Phytoremediation as a green biotechnology tool for emerging environmental pollution: a step forward towards sustainable rehabilitation of the environment. CHEM ENG J 415:129040
  19. Lee C, Sedlak DL (2008) Enhanced formation of oxidants from bimetallic nickel-iron nanoparticles in the presence of oxygen. Environ Sci Technol 42(22):8528–8533
  20. Lin H, Niu J, Xu J, Li Y, Pan Y, 2013. Electrochemical mineralization of sulfamethoxazole by Ti/SnO<sub>2</sub>-Sb/Ce-PbO<sub>2</sub> anode: kinetics, reaction pathways, and energy cost evolution. Electrochim. Acta 97, 167e174
  21. Liu X, Chen Zhengxian, Wang Qingping, 2012. Kaolin loaded nano-iron-nickel bimetal to remove azo dyes from water and direct sun-fast black G. Environmental Engineering Journal
  22. Liu Y, Chen S, Quan X, Yu H, Zhao H, Zhang Y (2015) Efficient mineralization of perfluorooctanoate by electro-Fenton with H<sub>2</sub>O<sub>2</sub> electro-generated on hierarchically porous carbon. Environ Sci Technol 49(22):13528e13533
  23. Lu LA, Xz B, Dan LA, Kang S, Qi D, & Yh, D., 2021. Occurrence and ecological risk assessment of ppcps in typical inflow rivers of Taihu Lake, China. J ENVIRON MANAGE, 285
  24. Lu Z, Zhou, Shaomin, Xu, & Yanling., 2017. High saturation magnetization superparamagnetic Fe/Ni core/shell microparticles for chromium removal. RSC Advances
  25. Meng Y, Liu W, Fiedler H, Zhang J, Zhang T (2021), Fate and risk assessment of emerging contaminants in reclaimed water production processes. FRONT ENV SCI ENG, 15(5)
  26. Younis MA, Lyu S, Lei C, Yang B, 2021. Efficient mineralization of sulfanilamide over oxygen vacancy-rich NiFe-LDH nanosheets array during electro-Fenton process. Chemosphere 268 et al (2021) 129272
  27. Pérez-Lemus N, López-Serna R, Pérez-Elvira et al (2019) Analytical methodologies for the determination of pharmaceuticals and personal care products (ppcps) in sewage sludge: a critical review - sciencedirect. Anal Chim Acta 1083:19–40
  28. Oller I, Malato S, & JA Sánchez-Pérez., 2012. Combination of advanced oxidation processes and biological treatments for wastewater decontamination—a review. SCI TOTAL ENVIRON, 409(20), 4141–4166
  29. Ren B, Geng J, Wang Y, Wang P 2021. Emission and ecological risk of pharmaceuticals and personal care products affected by tourism in Sanya City, China. ENVIRON GEOCHEM HLTH(2)

30. Samaras VG, Stasinakis AS, Mamais D, Thomaidis NS, Lekkas TD (2013) Fate of selected pharmaceuticals and synthetic endocrine disrupting compounds during wastewater treatment and sludge anaerobic digestion. *J. Hazard. Mater*, 244-245(JAN.15), 259-267
31. Schrick B, Blough JL, Jones AAD, Mallouk TE (2002) Hydrodechlorination of trichloroethylene to hydrocarbons using bimetallic nickeliron nanoparticles. *CHEM MATER*, 14(12)
32. Shahriar A, Tan J, Sharma P, Hanigan D, & Yang Y, 2021. Fate and human health impacts of pharmaceuticals and personal care products in reclaimed wastewater irrigation for agriculture. *ENVIRON POLLUT*, 116532
33. Shannon MA, Bonn PW, Elimelech M, Georgiadis JG, Marinas BJ, Mayes AM, 2008. Science and technology for water purification in the coming decades. *Nature*, 452(7185), 301–10
34. Shen B, Wen X Huang, X., 2017. Enhanced removal performance of estriol by a three-dimensional electrode reactor. *Chem. Eng. J.* 327, 597e607
35. Stasinakis AS, Thomaidis NS, Arvaniti OS, Asimakopoulos AG, Samaras VG & Ajibola, A., 2013. Contribution of primary and secondary treatment on the removal of benzothiazoles, benzotriazoles, endocrine disruptors, pharmaceuticals and perfluorinated compounds in a sewage treatment plant. *SCI TOTAL ENVIRON*, 463-464(oct.1), 1067-1075
36. Sun Lingfang, Yu Zebin, Peng Zhenbo, et al, 2014. Preparation of Fe-Ni-TiO<sub>2</sub>/AC particle electrode and visible light photoelectrocatalytic synergistic degradation of RhB. *China Environmental Science*. (12): 3119–3126
37. Tarpani R, Azapagic A (2018) Life cycle environmental impacts of advanced wastewater treatment techniques for removal of pharmaceuticals and personal care products (ppcps). *J ENVIRON MANAGE* 215(1):258–272
38. Wang T, Zhou Y, Cao S et al (2019), 2019. Degradation of sulfanilamide by Fenton-like reaction and optimization using response surface methodology. *Ecotoxicol Environ Saf* 172:334–340
39. Wang CT, Hu JL, Chou WL, Kuo YM (2008) Removal of color from real dyeing wastewater by electro-fenton technology using a three-dimensional graphite cathode. *J HAZARD MATER* 152(2):601–606
40. Wang D, Li H, Wu G, Guo R, Li L, Zhao C, Liu F, Wang Y (2017) Photoelectrocatalytic degradation of partially hydrolyzed polyacrylamide using a novel particle electrode. *RSC Adv* 7(87):55496–55503
41. Wang J, Wang S (2016) Removal of pharmaceuticals and personal care products (ppcps) from wastewater: a review. *J ENVIRON MANAGE* 182:620–640
42. Weng X, Qian S, Shen L, Chen Z, Megharaj M, & Naidu R (2014) Enhancement of catalytic degradation of amoxicillin in aqueous solution using clay supported bimetallic Fe/Ni nanoparticles. *Chemosphere* 103(may):80–85
43. Wenquan S, Yongjun S, Kinjal (2019) Electro-catalytic oxidation of tetracycline by Bi-Sn-Sb/γ-Al<sub>2</sub>O<sub>3</sub> three-dimensional particle electrode. *J HAZARD MATER*
44. Zhang X Zi Song, Huo Hao Ngo, Wen Shan Guo, Zumin Zhang, Yang Liu, Dan Zhang, Zhongliang Long. 2020. Impacts of typical pharmaceuticals and personal care products on the performance and

- microbial community of a sponge-based moving bed biofilm reactor. *Bioresource Technology*, 295, 122298
45. Xiong Y, Karlsson HT (2003) An experimental investigation of chemical oxygen demand removal from the wastewater containing oxalic acid using three-phase three-dimensional electrode reactor. *Adv Environ Res* 7(1):139–145
  46. Xu W, Zhang G, Zou S, Ling Z, Wang G, Yan W (2009) A preliminary investigation on the occurrence and distribution of antibiotics in the yellow river and its tributaries, china, vol 81. *Water Environment Research A Research Publication of the Water Environment Federation*, p 2483
  47. Yang L, Hao X, Yu D, Zhou P, Lai B (2021) High visible-light catalytic activity of bis-pdi-t@tio<sub>2</sub> for activating persulfate toward efficient degradation of carbamazepine. *SEP PURIF TECHNOL* 263(5):118384
  48. Yang L, Wang T, Zhou Y, Shi B, Meng J, 2020. Contamination, source and potential risks of pharmaceuticals and personal products (ppcps) in baiyangdian basin, an intensive human intervention area, china. *SCI TOTAL ENVIRON*, 760, 144080
  49. Yi Y, Yong SO, Kim KH, Kwon EE, Tsang YF (2017), Occurrences and removal of pharmaceuticals and personal care products (ppcps) in drinking water and water/sewage treatment plants: a review. *SCI TOTAL ENVIRON*, 596-597(OCT.15), 303-320
  50. Ying XA, Hw A, Lu LB, Meng RA, Hq A, Al A, 2021. A review of distribution and risk of pharmaceuticals and personal care products in the aquatic environment in china - sciencedirect. *ECOTOX ENVIRON SAFE*, 213
  51. Yxc A, Jc B, Dan WA, Ysl A, Yqy C, & Lxh, A., 2021. Highly enhanced biodegradation of pharmaceutical and personal care products in a novel tidal flow constructed wetland with baffle and plants - sciencedirect. *WATER RES*, 193
  52. Zhang X, Zhou Y, Zhao C, Sun Z, Zhang Z, Mirza ZA, Saylor G, Zhai J, Zheng H (2016) Electric field induced activated carbon fiber (ACF) cathode transition from an initiator/a promoter into an electrocatalyst in ozonation process. *Chem Eng J* 304:129–133
  53. Zhang L, Chen R, Liu Y, Deng Y, Li Z, Dong Y (2019) Influence of metal ions on sulfonamide antibiotics biochemical behavior in fiber coexisting system. *J. Environ. Sci*
  54. Zhang Z, Feng YN, Liu, Zhao Y, Qiu L (2020) Preparation of sn/mn loaded steel slag zeolite particle electrode and its removal effect on rhodamine b(rhb). *Journal of Water Process Engineering* 37:101417
  55. Zhao, Xin (2017) Preparation of activated carbon supported multi-component metal oxide composite material and its electrocatalytic oxidation of pollutants in water. *Beijing University of Chemical Technology*
  56. Yueguang Z, Qingfu Wang, Yonghe Sun et al, 2014. Study on structural properties of biochar under different materials and carbonized by ftir. *Spectroscopy and spectral analysis*, 34(4), 962
  57. Zhou S, Li Y, Chen J, Liu Z, Wang Z, Na P (2014) Enhanced cr(vi) removal from aqueous solutions using ni/fe bimetallic nanoparticles: characterization, kinetics and mechanism. *RSC Adv*

58. Zhu W, Liu J, Yu S, Zhou Y, Yan X (2016) Ag loaded WO<sub>3</sub> nanoplates for efficient photocatalytic degradation of sulfanilamide and their bactericidal effect under visible light irradiation. J Hazard Mater 318:407–416
59. Chen Z, Zhang Y, Zhou L, Zhu H, Wan F, Wang Y et al (2017) Performance of nitrogen-doped graphene aerogel particle electrodes for electro-catalytic oxidation of simulated bisphenol a wastewaters. J HAZARD MATER

## Figures

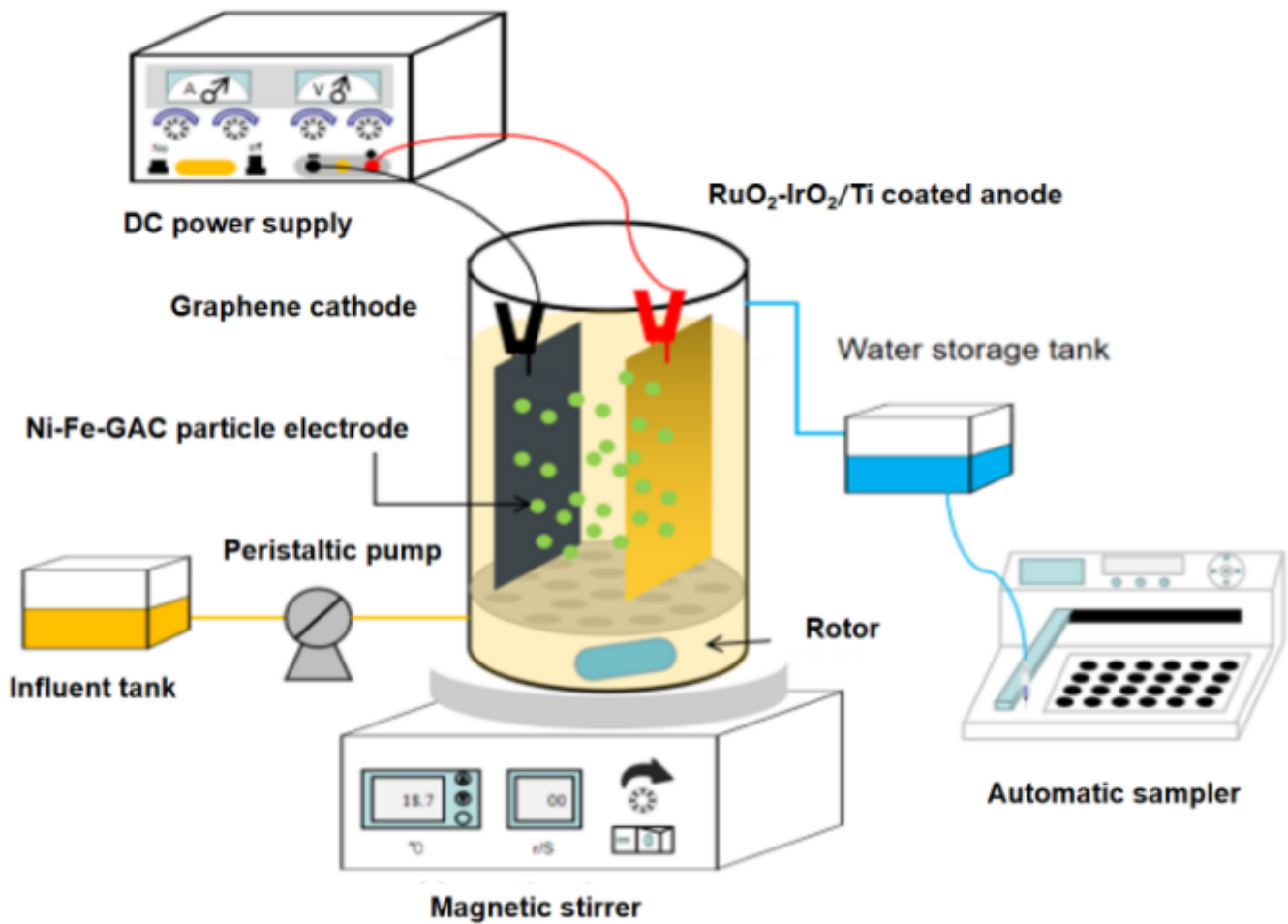
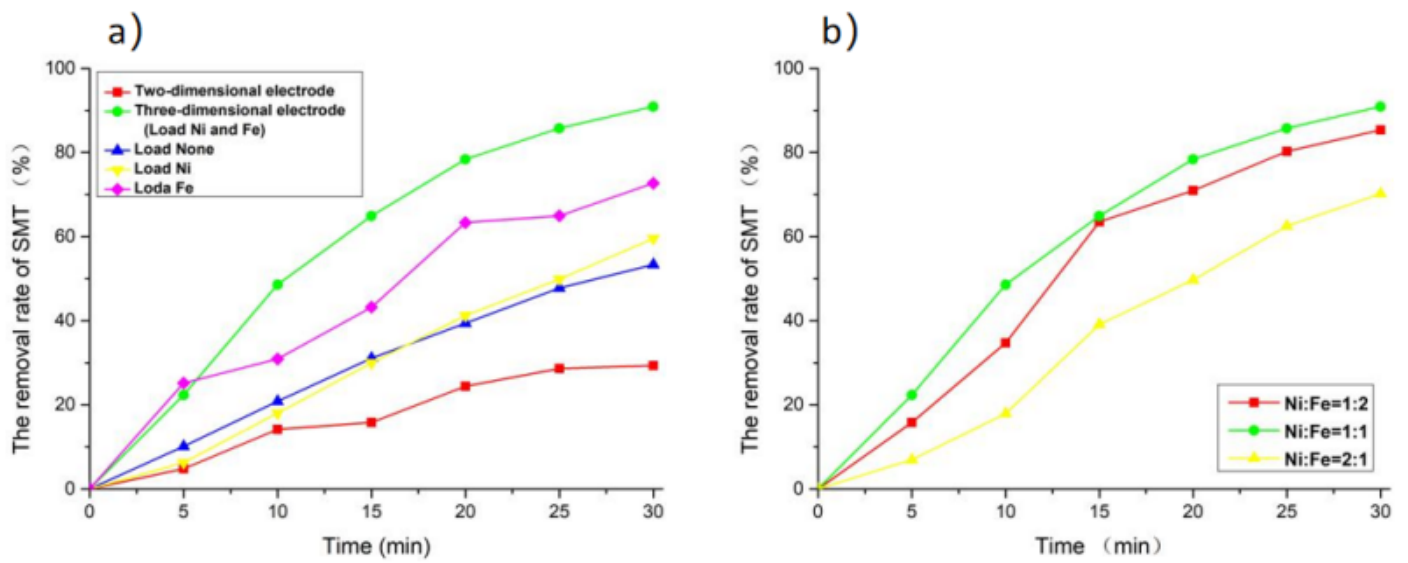


Figure 1

Three-dimensional electrode electrochemical reaction device



**Figure 2**

Effect on SMT removal rate: a) active component of particle electrode; b) Ni: Fe mass ratio of the particle electrode.

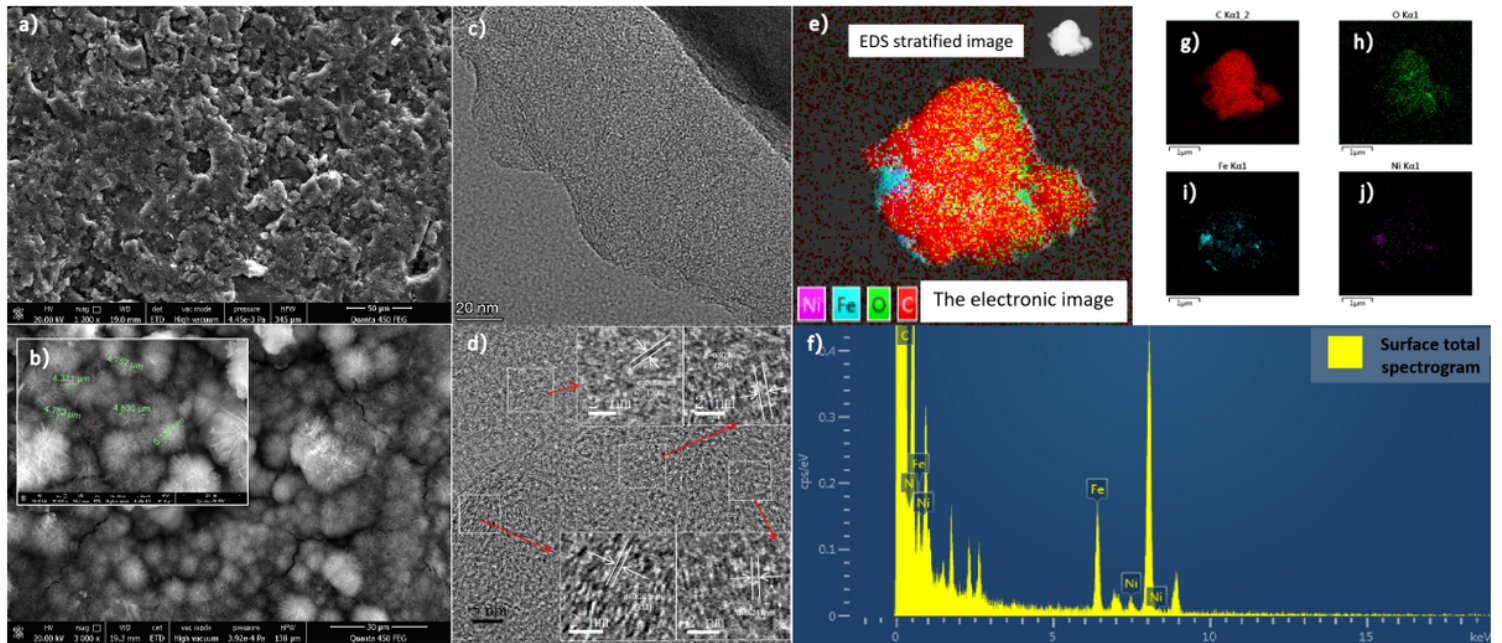


**Figure 3**

SEM photo of particle electrode a) GAC; b) GAC@Ni/Fe; c) TEM figure of GAC@Ni/Fe particle electrode; d) HRTEM figure of GAC@Ni/Fe particle electrode; e) element distribution diagram; f) EDS total area spectrum diagram; g)-j) carbon, oxygen, iron, nickel elements' distribution image of GAC@Ni /Fe particle electrode

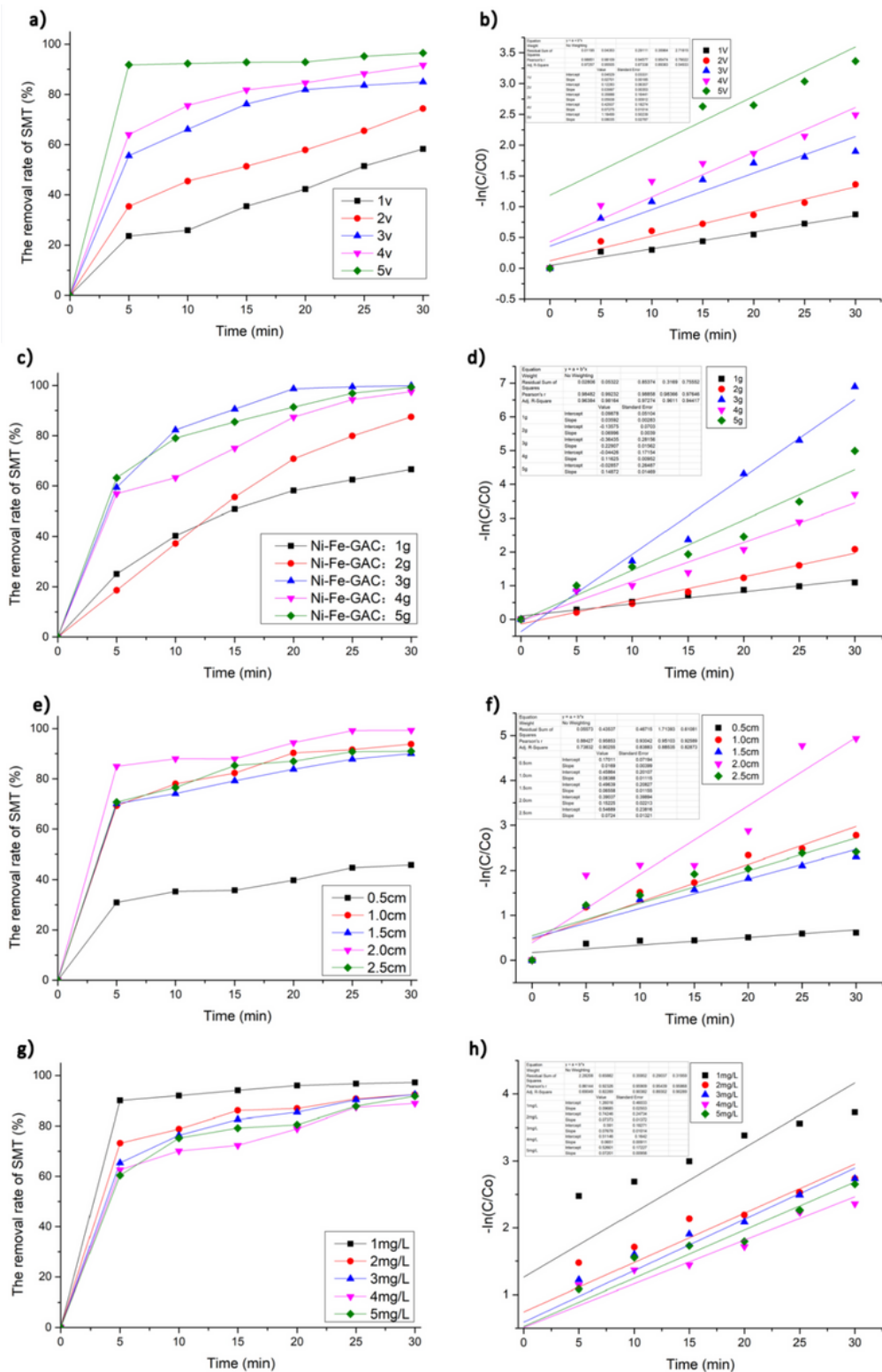


**Figure 4**

a) XRD figure of GAC and GAC@Ni/Fe particle electrode; XPS figure of Ni-Fe-CAG particle electrode: b) Full spectrum; c) Fe 2P; d) Ni 2P

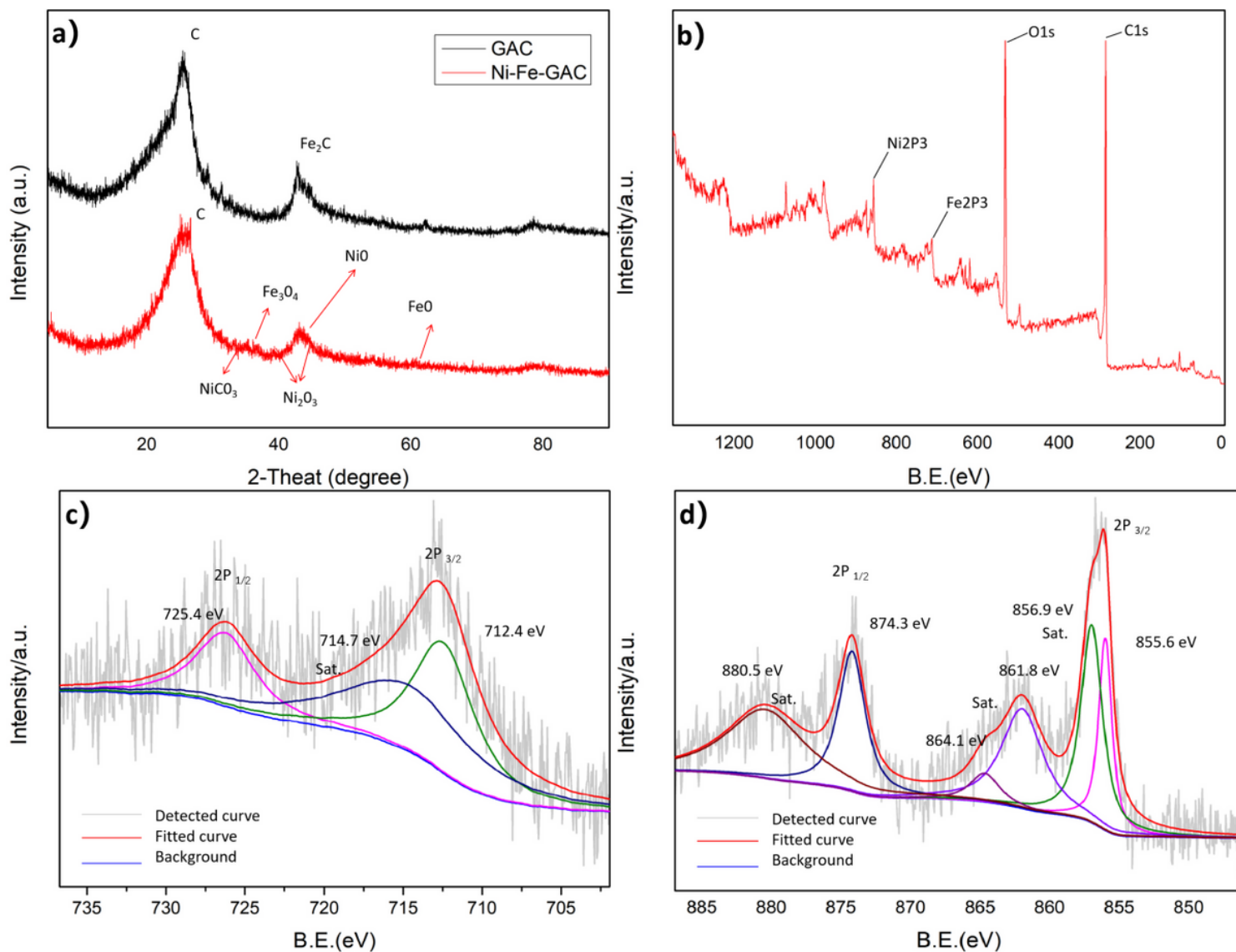


**Figure 5**

Effects of key factors on SMT removal rate and Simulation of reaction kinetics:(a-b)cell voltages, (c-d)particle electrode dosages,(e-f)electrode plate spacing,(g-h)pollutants initial concentration.

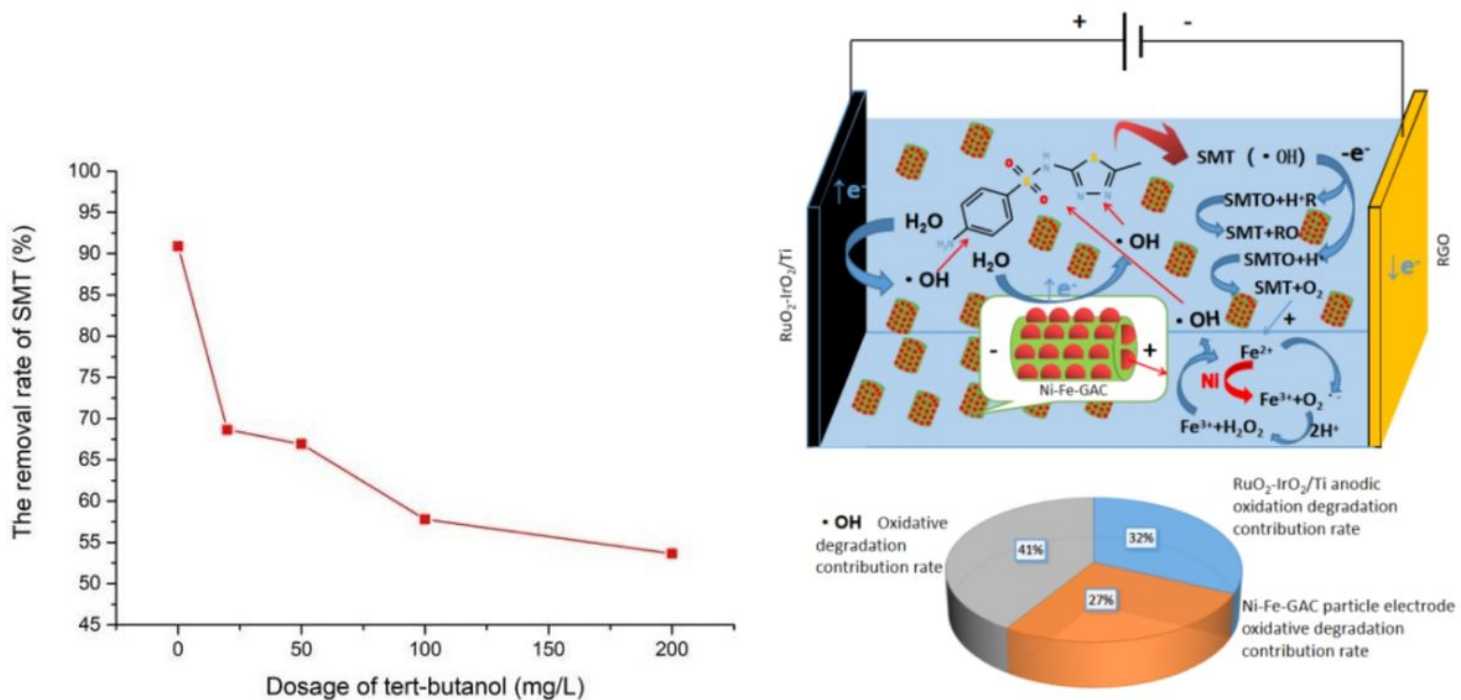


Figure 6

a) The effect of tert-butanol dosage on SMT degradation efficiency; b) Degradation mechanism and degradation contribution rate

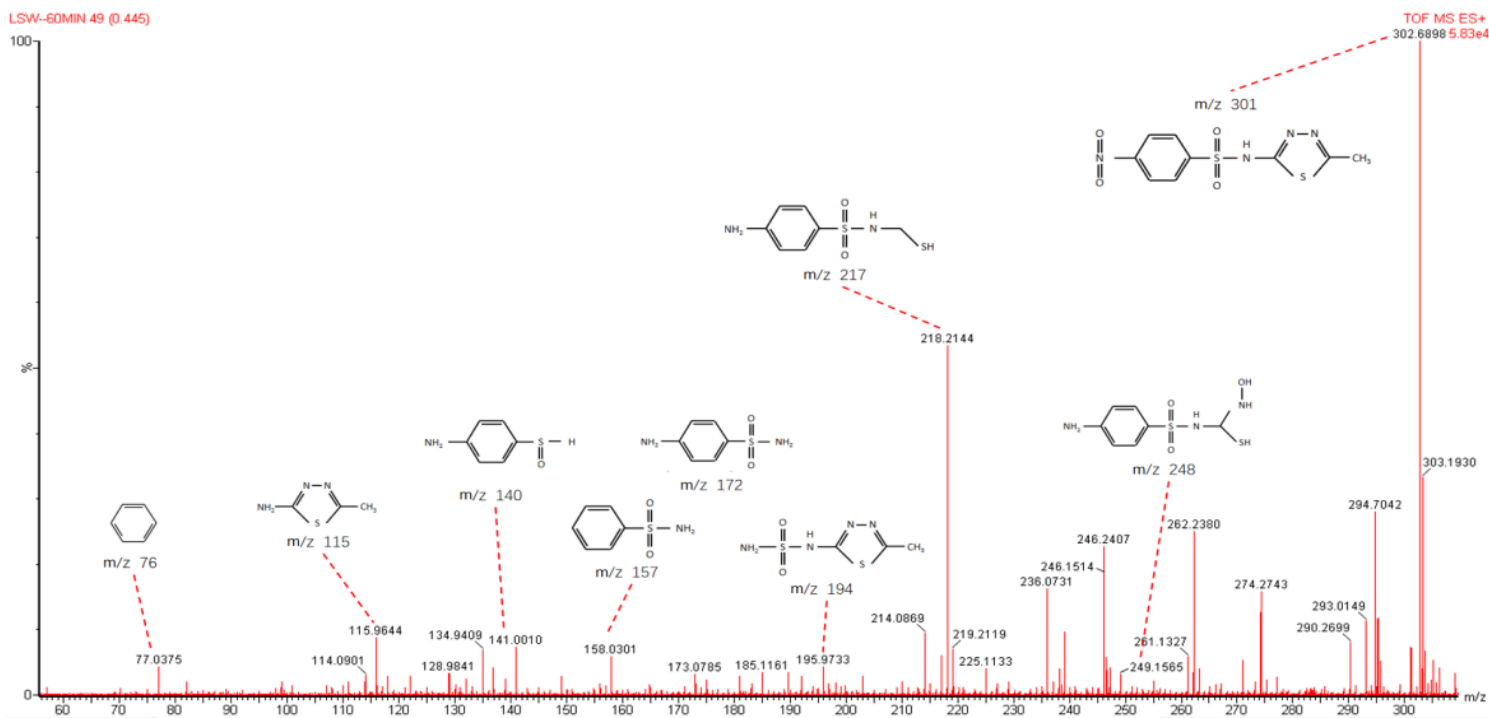
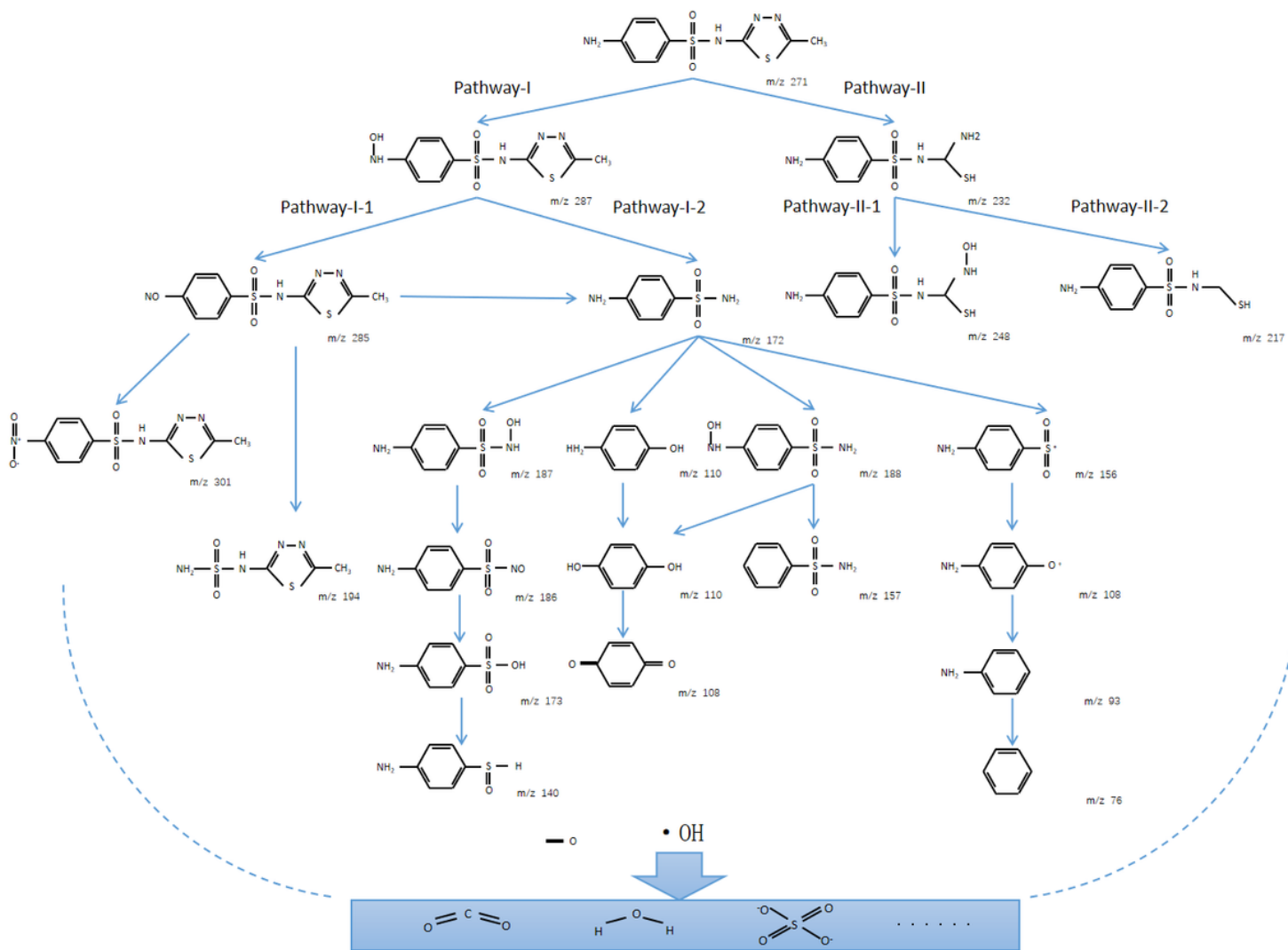


Figure 7

The main fragments and structural information of the intermediate products



**Figure 8**

Possible degradation pathways of SMT

## Supplementary Files

This is a list of supplementary files associated with this preprint. Click to download.

- [Supplementarymaterial.docx](#)